Am J Physiol Regul Integr Comp Physiol 322: R620–R628, 2022.
First published April 26, 2022; doi:10.1152/ajpregu.00034.2022

american physiological society

AMERICAN JOURNAL OF PHYSIOLOGY
REGULATORY, INTEGRATIVE AND COMPARATIVE PHYSIOLOGY

RESEARCH ARTICLE

Sympathetic transduction of blood pressure during graded lower body negative pressure in young healthy adults

Massimo Nardone,[1] Carlin Katerberg,[1] André L. Teixeira,[1] Jordan B. Lee,[1] Julian C. Bommarito,[1] and Philip J. Millar[1,2]

[1]*Department of Human Health and Nutritional Sciences, University of Guelph, Guelph, Ontario, Canada and* [2]*Toronto General Research Institute, Toronto General Hospital, Toronto, Ontario, Canada*

Abstract

Sympathetic transduction of blood pressure (BP) is correlated negatively with resting muscle sympathetic nerve activity (MSNA) in cross-sectional data, but the acute effects of increasing MSNA are unclear. Sixteen (4 female) healthy adults (26 ± 3 years) underwent continuous measurement of heart rate, BP, and MSNA at rest and during graded lower body negative pressure (LBNP) at −10, −20, and −30 mmHg. Sympathetic transduction of BP was quantified in the time (signal averaging) and frequency (MSNA-BP gain) domains. The proportions of MSNA bursts firing within each tertile of BP were calculated. As expected, LBNP increased MSNA burst frequency ($P < 0.01$) and burst amplitude ($P < 0.02$), although the proportions of MSNA bursts firing across each BP tertile remained stable (all $P > 0.44$). The MSNA-diastolic BP low-frequency transfer function gain ($P = 0.25$) was unchanged during LBNP; the spectral coherence was increased ($P = 0.03$). Signal-averaged sympathetic transduction of diastolic BP was unchanged (from 2.1 ± 1.0 at rest to 2.4 ± 1.5, 2.2 ± 1.3, and 2.3 ± 1.4 mmHg; $P = 0.43$) during LBNP, but diastolic BP responses following nonburst cardiac cycles progressively decreased (from −0.8 ± 0.4 at rest to −1.0 ± 0.6, −1.2 ± 0.6, and −1.6 ± 0.9 mmHg; $P < 0.01$). As a result, the difference between MSNA burst and nonburst diastolic BP responses was increased (from 2.9 ± 1.4 at rest to 3.4 ± 1.9, 3.4 ± 1.9, and 3.9 ± 2.1 mmHg; $P < 0.01$). In conclusion, acute increases in MSNA using LBNP did not alter traditional signal-averaged or frequency-domain measures of sympathetic transduction of BP or the proportion of MSNA bursts firing at different BP levels. The factors that determine changes in the firing of MSNA bursts relative to oscillations in BP require further investigation.

blood pressure; lower body negative pressure; muscle sympathetic nerve activity; sympathetic transduction

INTRODUCTION

The use of microneurography to directly record postganglionic muscle sympathetic nerve activity (MSNA) with high temporal resolution has been integral for providing insight toward the neural control of the circulation in humans (1). However, our understanding of sympathetic end-organ responsiveness, or the transduction of MSNA into changes in blood pressure (BP) or vascular conductance/resistance, is limited, owing to analytical challenges in quantifying the sympathetic neural signaling cascade. Efferent propagation of sympathetic outflow to synaptic terminals facilitates neurotransmitter efflux and bindings to postjunctional receptors, resulting in increased vasomotor tone (2, 3). However, integrating information on beat-to-beat neurotransmitter release and adrenergic receptor binding affinity and saturation kinetics remains technically unfeasible. As a result, analyses of sympathetic transduction in humans rely on signal-processing techniques of neural (input) and hemodynamic (output) signals in the time (i.e., signal-averaging) and the frequency (i.e., sensitivity of the BP-MSNA relationship using transfer function analyses) domain to isolate physiological responses from signal noise (2).

Using time-domain signal-averaging, our laboratory (4) and others (5–8) have demonstrated that tonic levels of resting MSNA are associated with sympathetic transduction of BP, such that individuals with higher resting MSNA present with lower sympathetic transduction (4, 5, 9, 10). We have shown that sympathetic transduction of BP is influenced by the prevailing BP level at which each MSNA burst fires, with burst discharge above the mean BP set-point displaying paradoxical reductions in BP (11). Individuals with higher resting MSNA have a larger proportion of sympathetic bursts firing above the mean BP set-point, which arithmetically drives the lower peak BP transduction (11). Whether these findings are a result of methodological constraints of the signal-averaging method (i.e., fewer bursts occurring in isolation) or physiological differences in end-organ responsiveness related to neurotransmitter release or adrenergic receptor sensitivity remains unclear (4, 12–14), but they suggest that sympathetic transduction is impacted by baroreflex-mediated BP-MSNA coupling to appropriately synchronize sympathetic burst firing to oscillations in BP. Unfortunately, confirmation of cross-sectional associations using within-participant designs to investigate the impact of reflex changes in sympathetic activity on resting

Correspondence: P. J. Millar (pmillar@uoguelph.ca).
Submitted 15 February 2022 / Revised 14 April 2022 / Accepted 17 April 2022

sympathetic transduction is limited (8, 15). Exposure to high altitude increased resting MSNA and decreased resting sympathetic transduction of BP (8), whereas exposure to hyperoxia in patients with obstructive sleep apnea decreased resting MSNA but did not alter resting sympathetic transduction of BP (15). Thus, it remains unclear whether reflex modulation of sympathetic activity influences arterial baroreflex control of MSNA burst occurrence, which could subsequently impact the proportion of MSNA bursts firing above the mean BP set-point, BP-MSNA coherence, and sympathetic transduction responsiveness.

Lower body negative pressure (LBNP) elicits baroreflex-mediated increases in sympathetic outflow while minimally perturbing resting hemodynamics (16), representing a useful model to evaluate reflex control of sympathetic transduction. Prior work has demonstrated increased MSNA burst frequency, amplitude, and burst clustering (16–18), whereas analyses of low-frequency oscillations in BP and MSNA have shown increased spectral power of BP and MSNA, along with their respective signal coherence (17–21). However, the extent to which changes in low-frequency oscillations in MSNA and diastolic BP during reflex increases in MSNA translate into changes in signal-averaged sympathetic transduction has not been evaluated to date.

The objective of the current study is to evaluate the influence of acute elevations in MSNA on signal-averaged sympathetic transduction of BP in young healthy adults. As supported by cross-sectional work (11), we hypothesize that sympathetic transduction of BP will decrease during LBNP-induced elevations in MSNA, secondary to an increased proportion of MSNA bursts firing above the BP set-point.

METHODS

Participants

Sixteen (4 female) young healthy participants were recruited for this study. Participants were all nonobese and normotensive and self-reported to be free from any cardiovascular, metabolic, or neurological conditions. Menstrual cycle was uncontrolled in three female participants, with the remaining female participant having a hormonal intrauterine device. Participants identified as white/European (n=11), white/European and Southeast Asian (n=2), white/European and South Asian (n=1), white/European and Latin American (n=1), and South Asian (n=1). All research protocols were approved by the University of Guelph research ethics board, and all participants completed written informed consent before testing.

Experimental Protocol

Prior to the study visit, participants refrained from caffeine, alcohol, and strenuous exercise for 24 h. Participants were positioned supine in a custom-designed lower body pressure tank, which was sealed to the participants at the level of the iliac crest (22). A calibrated pressure gauge (American Sensor Technologies, Inc, Mt. Olive, NJ) monitored the internal pressure of the lower body pressure tank, which was manipulated using a modified vacuum motor. Following instrumentation and acquisition of a microneurographic recording, participants rested for 5–10 min to ensure stabilization of the MSNA recording site. Participants then underwent an 8-min baseline, followed by a graded LBNP protocol consisting of 8-min stages at −10, −20, and −30 mmHg. Each 10-mmHg reduction in LBNP was achieved across a 45- to 60-s period, to minimize rapid changes in BP and participant movement, which could alter the MSNA recording site.

Measurements

Discrete blood pressure was measured from the left arm by an automated oscillometric device (BPTru Medical Devices, Coquitlam, BC, Canada). At minute 2 of each stage, four consecutive measurements were taken and averaged. Respiratory excursions were measured using a piezoelectric transducer placed around the upper abdomen (Pneumotrace II. Morro Bay, CA). Beat-to-beat heart rate and blood pressure were measured using single-lead electrocardiography (ADInstruments, Australia) and finger photoplethysmography (Finometer MIDI, Finapres, the Netherlands), respectively. Beat-to-beat cardiac output (CO) was calculated using the Windkessel model (noninvasive cardiac output extension, ADInstruments, New South Wales, Australia), whereas beat-to-beat total vascular conductance (TVC) was subsequently calculated as the quotient of CO and mean arterial pressure.

During the last 2 min of each stage, brachial artery blood flow was quantified with Duplex ultrasound (Vivid q; General Electric, Boston, MA) using a linear-array probe operating at 13 MHz and 5 MHz for B-mode and Doppler, respectively. Arterial diameter and blood velocity profiles were captured and stored on a computer using the DVI2USB 3.0 video grabber (Epiphan System, Ottawa, ON, Canada), which were then analyzed with an offline semiautomated analysis program (Cardiovascular Suite; Quipu, Pisa, Italy). Brachial artery diameter and mean blood flow velocity were calculated in 1-s bins, with a 1-min stable recording being averaged to derive brachial artery diameter and mean velocity, as previously described (23). Brachial blood flow was subsequently calculated as follows: blood flow (mL/min) = (MBV) × (πr^2) × 60, where MBV is mean blood flow (cm/s), and r (cm) is the radius of the brachial artery. Forearm vascular conductance (FVC) was calculated as the quotient of brachial artery blood flow and mean arterial pressure.

Efferent multiunit muscle sympathetic nerve activity (MSNA) was collected, as described previously (24). A high-impedance tungsten microelectrode was inserted posterior to the fibular head, into the common peroneal nerve, whereas a low-impedance reference electrode was inserted ∼3–4 cm away, beneath the surface of the skin. Confirmation of muscle sympathetic activity was based on the presence of spontaneously occurring, triangular-shaped bursts of activity that were aligned with the cardiac cycle; activation to an end-expiratory apnea; and the lack of responsiveness to skin stroking or an auditory perturbation. The raw MSNA neurogram was amplified (75,000×), bandpass filtered (0.7–2.0 kHz), rectified, and integrated using a 0.1-s time constant to generate the integrated MSNA neurogram (Nerve Traffic Analyzer, Model 662 C-4; University of Iowa, Iowa City, IA). MSNA neurograms were analyzed in a semiautomated custom LabVIEW program (National Instruments, Austin, TX). Determination of a sympathetic burst was based on a 3:1 signal-to-noise ratio and alignment with the time-shifted cardiac cycle. The largest MSNA burst within the baseline recording was normalized to a value of 100% to control for interindividual differences in electrode proximity to the sympathetic nerve bundles.

MSNA burst frequency (bursts/min), burst incidence (bursts/100 heartbeats), normalized burst amplitude (%), and total MSNA (au) were computed.

Data Analysis

All data were digitized and stored using LabChart (v. 8; PowerLab, ADInstruments, New South Wales, Australia) at a sampling frequency of 1 kHz, except for the raw MSNA neurogram, which was sampled at 20 kHz. The first minute of each stage was not analyzed to allow steady state to be reestablished, and therefore, all continuously collected hemodynamics and neural parameters were averaged across the last 7 min of each stage.

Sympathetic transduction of diastolic BP, MAP, and TVC were quantified using time-domain signal-averaged sympathetic transduction as previously described (4, 11, 25). Changes in hemodynamic parameters were serially tracked across 15 cardiac cycles for each heartbeat. Initiating cardiac cycles were categorized based on the presence or absence of an MSNA burst, and changes in hemodynamics were subsequently averaged across each serial time, respectively. Using the computed averages, resting sympathetic transduction was defined by the peak diastolic BP and nadir TVC response, whereas hemodynamic responses to nonburst cardiac cycles were defined by the nadir diastolic BP and peak TVC change. Quartiles of MSNA burst amplitude and the respective peak rise in diastolic BP were subsequently computed. Sympathetic transduction of diastolic BP was also quantified as the difference between the burst and nonburst responses (11) and after normalizing for MSNA burst frequency (peak Δ diastolic BP/MSNA burst frequency$^{-0.55}$) (4). Finally, tertiles of diastolic BP were computed and used to determine whether MSNA bursts fired when diastolic BP was below, around, or above the operating pressure (OP, or mean BP set-point). The proportions of MSNA bursts firing within each tertile were quantified as follows: (number of MSNA bursts firing within the respective tertile)/(total number of MSNA bursts).

Sympathetic transduction was also quantified using the MSNA-diastolic BP transfer function gain and coherence using a custom LabVIEW program (National Instruments, Austin, TX) (26). Following analysis of the sympathetic neurogram, beat-to-beat diastolic BP and normalized MSNA burst amplitudes were time aligned to the ECG R-wave. Cardiac cycles without an MSNA burst were denoted by a value of zero, whereas cardiac cycles with respective MSNA bursts were denoted by the normalized burst amplitude. The timing of sympathetic bursts was then advanced forward based on the average t-shift to ensure proper phase alignment. Seven minutes of nonequidistant beat-to-beat diastolic BP and MSNA were spline interpolated and resampled at 10 Hz. A total of 4,096 datapoints were submitted to a fast Fourier transformation, subdivided into seven overlapping segments, each containing 1,024 datapoints with 50% overlap using a Blackman–Harris window. The linear trend within each segment was removed. The auto-spectrum and cross-spectrum were quantified across three distinct frequency bands: very low frequency (VLF: 0–0.04 Hz), low frequency (LF: 0.04–0.15 Hz), and high frequency (HF: 0.15–0.50 Hz). The transfer function gain and coherence were then calculated with MSNA as the input variable and diastolic BP as the output variable. All participants presented with MSNA-diastolic BP LF coherence >0.4. Since lower coherence (<0.5) between MSNA and diastolic BP could represent true physiological differences rather than failure of the analytical technique (27), spectral estimates of the MSNA-diastolic BP LF gain were computed in all participants irrespective of the MSNA-diastolic BP LF coherence.

Arterial baroreflex control of MSNA was also quantified using the baroreflex threshold method (28, 29). Diastolic BPs were grouped into 3-mmHg bins, and the slope of the weighted linear regression between diastolic BP and MSNA burst occurrence was computed. All participants presented with Pearson's covariate coefficients >0.5 and ≥5 bins of diastolic BP. All bins containing saturation points (i.e., 0% and 100% burst incidences) were included in the computation of the regression slope. Lastly, as an exploratory analysis, the transfer function gain and coherence of respiratory excursions (input) and MSNA (output) or diastolic BP (output) were also computed.

Statistical Analysis

All analyses were conducted using RStudio version 1.4.1103 (30). Changes in hemodynamic, respiratory, and sympathetic parameters across graded LBNP were statistically compared by linear mixed-effect modeling using the lme4 (31) and lmerTest (32) statistical packages. The LBNP stage (0, −10, −20, −30) was included as a fixed factor, whereas participants were included as a random effect to control for correlations within participants. When appropriate, post hoc analyses were conducted to evaluate changes from baseline using the emmeans (33) statistical package using a Tukey adjustment for multiple comparisons. To evaluate the effect of changes in MSNA burst amplitude on sympathetic transduction, MSNA burst quartile was included as a second fixed factor in the linear mixed effect model. Statistical significance was defined as $P < 0.05$. Data are presented as means ± SD.

RESULTS

The mean age and body mass index were 26 ± 3 yr and 26 ± 3 kg/m^2, respectively. All participants completed the −10 and −20 mmHg LBNP stages; however, the MSNA signal was lost in two male participants during −30 mmHg. During each stage of LBNP, diastolic BP (mean differences ± SD [range]: −0.7 ± 1.8 [−4.2–2.1], 0.4 ± 1.8 [−4.3–3.7], and −0.5 ± 1.5 [−2.8–2.1] mmHg, all $P > 0.17$) and MSNA burst frequency (−0.5 ± 4.1 [−9.0–5.0], 0.5 ± 4.0 [−7.0–6.5], and −0.4 ± 3.5 [−8.0–4.0] bursts/min, all $P > 0.63$) were similar during the first 2 min compared with the last 2 min, demonstrating achievement of steady-state perturbations. No participant experienced any symptoms of presyncope during the LBNP protocol.

Hemodynamic, Respiratory, and Sympathetic Responses to Graded Lower Body Negative Pressure

A representative tracing of 60-s beat-to-beat heart rate, blood pressure, and MSNA data across each LBNP stage is shown in Fig. 1*A*. Group-level data are presented in Table 1. Systolic BP, breathing frequency, and breathing depth were not different during graded LBNP (all $P > 0.11$). Diastolic BP, mean arterial pressure, and heart rate increased

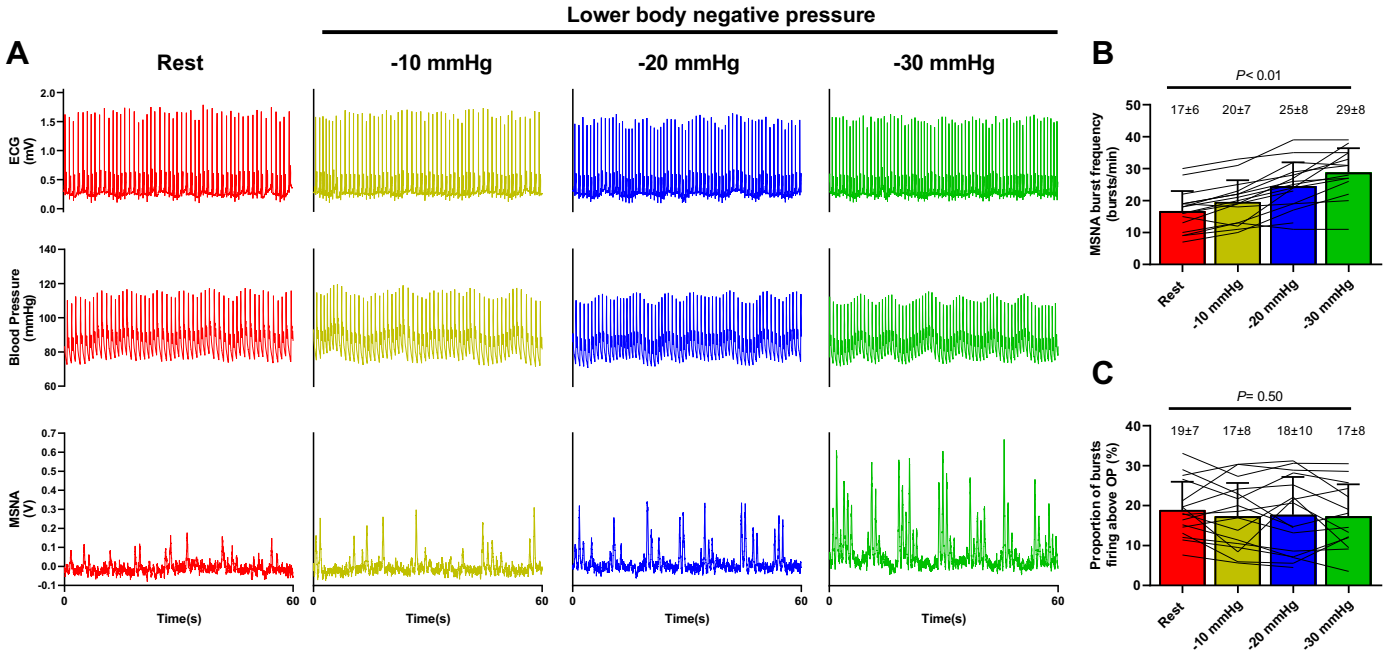

Figure 1. Representative 1-min recording of beat-to-beat heart rate (ECG), blood pressure (BP), and muscle sympathetic nerve activity (MSNA) at rest and during −10, −20, −30 mmHg of lower body negative pressure (*A*). Muscle sympathetic nerve activity (MSNA) burst frequency (*B*) and proportion of MSNA bursts firing above the operating pressure (*C*) at rest and during −10, −20, and −30 mmHg of lower body negative pressure in 16 (12 male, 4 female) participants. Red, yellow, blue, and green represent rest, −10 mmHg, −20 mmHg, and −30mmHg, respectively. Statistical analyses conducted using mixed-effect linear modeling.

(all $P < 0.046$), whereas stroke volume, cardiac output, brachial arterial blood flow, and FVC decreased, during graded LBNP (all $P < 0.03$). However, despite increased MSNA burst frequency during LBNP ($P < 0.01$, Fig. 1*B*), the proportions of MSNA bursts firing above ($P = 0.50$; Fig. 1*C*), below (from 48 ± 9 to 48 ± 9, 50 ± 10, and 49 ± 9%; $P = 0.69$), or around (from 33 ± 4 to 35 ± 4, 33 ± 4, and 34 ± 3%; $P = 0.44$) the OP were not different. MSNA burst incidence, normalized burst amplitude, and total MSNA were also increased during graded LBNP (all $P < 0.02$).

Sympathetic Transduction to Graded Lower Body Negative Pressure

Signal-averaged sympathetic transduction responses of diastolic BP and TVC are presented in Fig. 2, *A* and *D*, respectively. Sympathetic transduction of diastolic BP was unaltered during graded LBNP ($P = 0.43$; Fig. 2*B*). Larger MSNA bursts resulted in expected larger rises in diastolic BP (burst quartile fixed effect: $P < 0.01$); however, LBNP did not alter sympathetic transduction of diastolic BP across each quartile (LBNP

Table 1. *Hemodynamic, respiratory, and sympathetic responses to graded LBNP*

Variable	Rest (*n* = 16)	LBNP −10 mmHg (*n* = 16)	LBNP −20 mmHg (*n* = 16)	LBNP −30 mmHg (*n* = 14)	*P*
Hemodynamics					
Systolic BP, mmHg	111 ± 8	111 ± 9	111 ± 10	111 ± 11	0.981
Diastolic BP, mmHg	64 ± 8	65 ± 8	66 ± 8	67 ± 9*	<0.01
Mean arterial pressure, mmHg	80 ± 7	80 ± 7	81 ± 7	82 ± 9*	0.046
Heart rate, beats/min	60 ± 9	61 ± 9	65 ± 10*	69 ± 11*	<0.01
Stroke volume, mL	85 ± 14	83 ± 15	76 ± 15*	68 ± 15*	<0.01
Cardiac output, (L/min)	5.0 ± 1.0	5.0 ± 0.9	4.8 ± 0.9	4.6 ± 0.9*	0.03
Brachial artery blood flow, mL/min	58 ± 29	46 ± 22*	46 ± 22*	39 ± 24*	<0.01
FVC, mL/min/mmHg	0.74 ± 0.37	0.59 ± 0.27*	0.59 ± 0.26*	0.52 ± 0.31*	<0.01
Respiration					
Breathing frequency, breaths/min	15 ± 3	14 ± 3	15 ± 4	15 ± 4	0.11
Breathing depth, % of baseline	100 ± 0	116 ± 63	114 ± 72	111 ± 61	0.65
MSNA					
Burst incidence, bursts/100 heartbeats	29 ± 11	33 ± 12	39 ± 13*	43 ± 15*	<0.01
Normalized burst amplitude, %)	41 ± 6	49 ± 21	53 ± 28*	57 ± 27*	0.02
Total MSNA (au)	673 ± 246	968 ± 562	1,337 ± 946*	1,677 ± 990*	<0.01

*Significantly different from rest ($P < 0.05$). Statistical analyses conducted using mixed-effect linear modeling. Means ± SD. BP, blood pressure; FVC, forearm vascular conductance; LBNP, lower body negative pressure; MSNA, muscle sympathetic nerve activity.

fixed effect: $P = 0.17$). The nadir diastolic BP response following nonburst cardiac cycles progressively increased during LBNP ($P < 0.01$; Fig. 2*C*), and as a result, the difference in diastolic BP responses following MSNA burst and nonburst cardiac cycles was increased (from 2.9 ± 1.4 to 3.4 ± 1.9, 3.4 ± 1.9, and 3.9 ± 2.1 mmHg; $P < 0.01$). Normalized sympathetic transduction of diastolic BP was also increased during graded LBNP (from 9.4 ± 4.9 to 11.6 ± 7.0, 12.6 ± 8.0, and 14.3 ± 9.2; $P < 0.01$). Similar findings were observed with sympathetic transduction of MAP, such that the sympathetic transduction of MAP was unaltered (from 2.3 ± 1.1 to 2.5 ± 1.4, 2.3 ± 1.4, and 2.2 ± 1.3 mmHg; $P = 0.86$), whereas the nadir MAP response following nonburst cardiac cycles progressively increased (from −0.9 ± 0.4 to −1.1 ± 0.5, −1.2 ± 0.6, and −1.5 ± 0.8 mmHg; $P < 0.01$) during LBNP. Consistent with these observations, sympathetic transduction of TVC was unaltered ($P = 0.33$; Fig. 2*E*), whereas the peak TVC during nonburst cardiac cycles progressively increased ($P < 0.01$, Fig. 2*F*).

MSNA and Diastolic BP Oscillations during Graded LBNP

MSNA and diastolic BP spectral power and the MSNA-diastolic BP transfer function gain and coherence are presented in Table 2. Graded LBNP increased LF spectral power of MSNA ($P = 0.02$) and diastolic BP ($P = 0.047$). MSNA-diastolic BP gain was unchanged across all frequency bands (VLF: $P = 0.36$; LF: $P = 0.25$; HF: $P = 0.77$), whereas the MSNA-diastolic BP LF coherence was increased ($P = 0.03$). MSNA-diastolic BP LF gain was also unchanged during LBNP after excluding participants with a MSNA-diastolic BP LF coherence below 0.50 ($n = 4$; $P = 0.21$). At rest, the proportion of MSNA bursts firing above the OP was negatively associated with both signal-averaged sympathetic transduction of diastolic BP ($r = −0.76$; $P < 0.01$) and the MSNA-diastolic BP LF gain ($r = −0.63$; $P < 0.01$). Furthermore, signal-averaged sympathetic transduction of diastolic BP ($r = 0.84$; $P < 0.01$) and the difference between bursts and nonbursts ($r = 0.81$; $P < 0.01$) were both associated with the MSNA-diastolic BP LF gain.

Proportion of Bursts Firing above the OP and Sympathetic Transduction of BP and TVC

The change in the proportion of MSNA bursts firing above the OP was negatively associated with the change in signal-averaged sympathetic transduction of diastolic BP across each stage of LBNP ($r = −0.74$, −0.67, and −0.89, all $P < 0.01$; Fig. 3*A*), as well as the change in signal-averaged sympathetic transduction of TVC during −10 mmHg ($r = −0.60$; $P = 0.01$) and −30 mmHg ($r = −0.78$; $P < 0.01$) but not −20 mmHg ($r = −0.17$; $P = 0.53$; Fig. 3*B*; removal of outlier: $r = −0.59$; $P = 0.02$). Finally, the change in the proportion of MSNA bursts firing above OP was negatively associated with the change in MSNA-diastolic BP LF gain ($r = −0.85$; $P < 0.01$) at −30 mmHg but not at −10 ($r = −0.16$; $P = 0.55$) or −20 mmHg ($r = −0.06$; $P = 0.83$).

Modulating Effects of Sympathetic Baroreflex Sensitivity and Respiration

Sympathetic baroreflex sensitivity was unchanged during graded LBNP (from −4.1 ± 1.7 to −4.1 ± 1.1, −4.9 ± 1.9, and −4.6 ± 1.7 bursts/100 heartbeats/mmHg; $P = 0.19$). The change in baroreflex sensitivity was not correlated to the

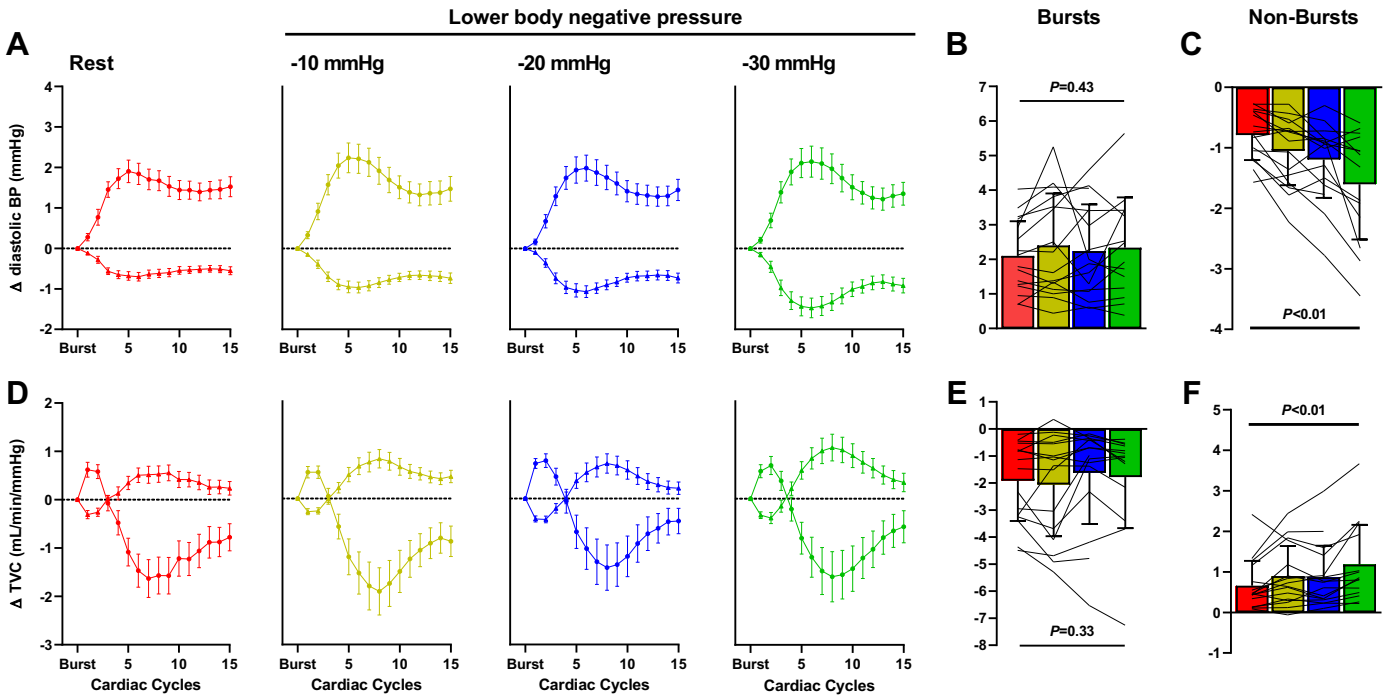

Figure 2. Signal-averaged sympathetic transduction at rest and during −10, −20, and −30 mmHg of lower body negative pressure in 16 (12 male, 4 female) participants. Diastolic BP transduction responses (*A*), peak Δ diastolic BP to sympathetic bursts (*B*), and nadir Δ diastolic BP to nonburst cardiac cycles (*C*). Total vascular conductance (TVC) transduction responses (*D*), nadir Δ TVC to sympathetic bursts (*E*), and peak Δ TVC to nonburst cardiac cycles (*F*). Red, yellow, blue, and green represent rest, −10 mmHg, −20 mmHg, and −30 mmHg, respectively. Statistical analyses conducted using mixed-effect linear modeling.

Table 2. *MSNA and diastolic BP spectral power and MSNA-diastolic BP transfer function gain and coherence during graded LBNP*

Variable	Rest (n = 16)	LBNP −10 mmHg (n = 16)	LBNP −20 mmHg (n = 16)	LBNP −30 mmHg (n = 14)	P
MSNA power, au^2					
VLF	19.1 ± 11.4	16.8 ± 8.3	16.9 ± 12.1	16.4 ± 10.9	0.80
LF	109.7 ± 47.4	143.4 ± 60.0	170.4 ± 115.8	201.5 ± 141.8*	0.02
HF	236.7 ± 81.4	289.6 ± 136.4	355.9 ± 203.3	489.9 ± 283.2*	<0.01
LF/HF	0.47 ± 0.15	0.53 ± 0.15	0.51 ± 0.20	0.47 ± 0.26	0.39
Diastolic BP power, mmHg^2					
VLF	4.6 ± 3.5	4.3 ± 3.7	3.2 ± 1.8	3.2 ± 2.8	0.37
LF	3.8 ± 2.6	4.8 ± 3.6	4.6 ± 2.7	5.7 ± 3.7*	0.047
HF	0.93 ± 0.56	0.95 ± 0.58	0.99 ± 0.53	1.18 ± 0.58	0.09
LF/HF	4.3 ± 2.6	5.3 ± 3.0	5.4 ± 3.5	5.4 ± 3.2	0.10
Gain, au/mmHg^2					
VLF	0.376 ± 0.239	0.348 ± 0.205	0.272 ± 0.182	0.329 ± 0.323	0.36
LF	0.146 ± 0.077	0.145 ± 0.067	0.154 ± 0.066	0.156 ± 0.077	0.25
HF	0.027 ± 0.007	0.025 ± 0.009	0.025 ± 0.009	0.026 ± 0.014	0.77
Coherence					
VLF	0.43 ± 0.14	0.40 ± 0.16	0.30 ± 0.11	0.33 ± 0.20	0.08
LF	0.59 ± 0.10	0.66 ± 0.12	0.66 ± 0.14	0.68 ± 0.16*	0.03
HF	0.26 ± 0.06	0.28 ± 0.08	0.28 ± 0.07	0.31 ± 0.10	0.25

*Significantly different from rest ($P < 0.05$). Statistical analyses conducted using mixed-effect linear modeling. Means ± SD. BP, blood pressure; HF, high frequency (0.15–0.5 Hz); LBNP, lower body negative pressure; LF, low frequency (0.04–0.15 Hz); MSNA, muscle sympathetic nerve activity; VLF, very low frequency (0–0.04 Hz).

changes in sympathetic transduction of diastolic BP across each stage of LBNP (r = −0.15–0.22; $P \geq 0.45$). Finally, at −30 mmHg of LBNP, the respiration-diastolic BP HF gain (from 0.02 ± 0.01 to 0.04 ± 0.03 au/mmHg; P = 0.047) and the respiration-MSNA HF gain (from 0.33 ± 0.2 to 0.63 ± 0.44 au/au; P = 0.02) and coherence (from 0.21 ± 0.05 to 0.29 ± 0.10; P = 0.02) were increased. The change in respiration-diastolic BP HF gain was correlated to the change in the sympathetic transduction of diastolic BP at −30 mmHg LBNP (r = 0.63, P = 0.02).

DISCUSSION

Cross-sectional studies have demonstrated that individuals with higher tonic MSNA have lower resting sympathetic

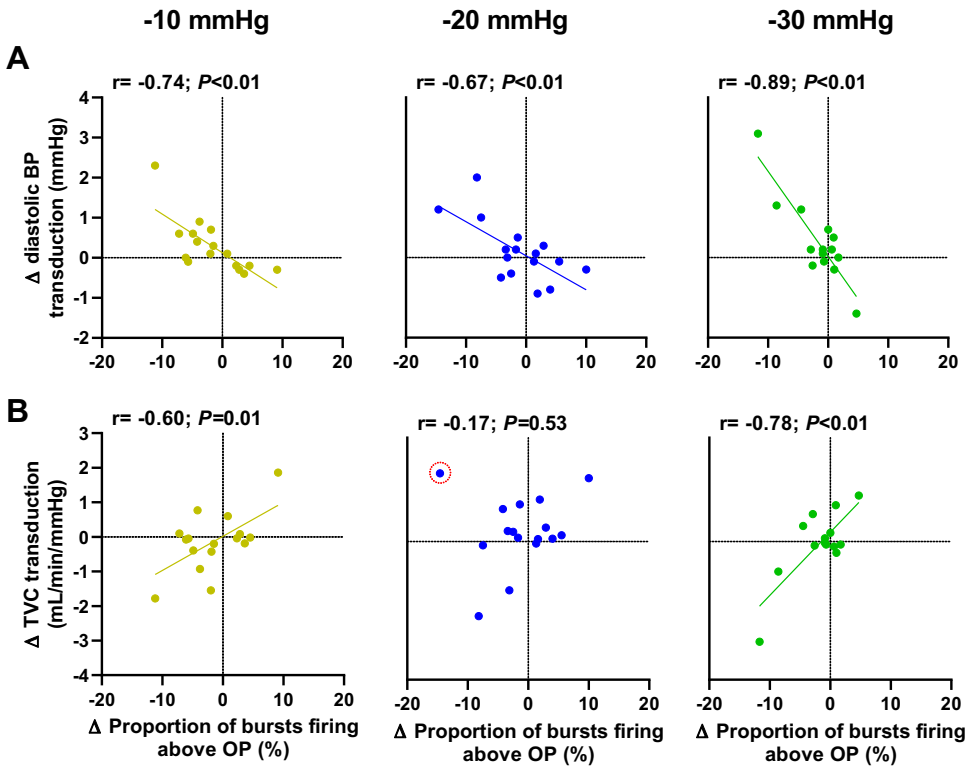

Figure 3. Correlations between the change in the proportion of sympathetic bursts firing above operating pressure (OP) and the change in sympathetic transduction of diastolic BP (*A*) or TVC (*B*) during −10, −20, and −30 mmHg of lower body negative pressure in 16 (12 male, 4 female) participants. Yellow, blue, and green represent −10 mmHg, −20 mmHg, and −30 mmHg, respectively. Statistical analyses conducted using Pearson bivariate correlations. Note: when the outlier from the middle figure of *B* is removed (highlighted by red circle), the Pearson bivariate correlation is r = −0.59 (P = 0.02).

transduction of BP (4–8); however, it is unclear whether similar findings are observed during within-participant studies eliciting reflex increases in sympathetic outflow. The present study yielded several novel findings. First, LBNP increased MSNA burst frequency and burst amplitude, but contrary to our hypothesis, did not alter the proportion of sympathetic bursts firing at different operating pressures, signal-averaged sympathetic transduction of diastolic BP, MAP, and TVC, or the MSNA-diastolic BP LF gain. Second, diastolic BP and TVC responses following nonburst cardiac cycles progressively increased during graded LBNP, such that the differences in hemodynamic responses between MSNA burst and nonburst cardiac cycles were increased. Third, the change in the proportion of MSNA bursts firing above the OP was strongly associated with both the change in signal-averaged sympathetic transduction of diastolic BP and the MSNA-diastolic BP LF gain. Fourth, strong positive relationships exist between resting signal-averaged sympathetic transduction of diastolic BP and the MSNA-diastolic BP LF gain. Collectively, these results provide novel insight toward the impact of acute increases in sympathetic outflow on sympathetic transduction of BP in young adults.

Most studies evaluating signal-averaged sympathetic transduction have focused on cross-sectional analyses exploring differences in sympathetic responsiveness across conditions such as aging, hypertension, diabetes mellitus, and pregnancy (10, 34–36). Studies exploring acute changes in sympathetic transduction using within-participant designs are limited but necessary to understanding the origin of the relationship with resting MSNA. For example, exposure to high altitude in lowlanders increased resting MSNA, enhanced the drop in BP following nonburst cardiac cycles, and decreased the sympathetic transduction slope (8), independent of changes in sympathetic baroreflex sensitivity (37). Statistical adjustment for the changes in MSNA abolished the attenuation of the sympathetic transduction slope (8). In contrast, exposure to hyperoxia in patients with obstructive sleep apnea decreased MSNA but did not alter BP responses following MSNA bursts, nonburst cardiac cycles, the sympathetic transduction slope, or sympathetic baroreflex sensitivity (15). The current work, in a cohort of healthy young adults, unaffected by disease or environmental conditions, is the first to examine the effects of acute graded increases in MSNA on measures of sympathetic transduction.

Using the commonly assessed signal-averaged peak diastolic BP response following an MSNA burst as a measure of sympathetic transduction (2), we observed no change across each level of LBNP. These findings were consistent during low levels of LBNP (−10 mmHg), when sympathetic outflow is selectively increased without a concomitant change in hemodynamics, and during higher levels of LBNP (−30 mmHg), when robust increases in sympathetic outflow can influence BP, arguing against a confounding influence of BP on transduction outcomes. Although not expected, this result is not surprising, given that LBNP increased MSNA without causing a shift in the proportion of MSNA bursts firing above the OP. Our previous work found that signal-averaged sympathetic transduction of BP is strongly correlated with the proportion of MSNA bursts occurring above the OP, owing to the fact that these bursts are associated with paradoxical reductions in BP (11). The apparent lack of change in sympathetic transduction of BP was also observed in the frequency-domain analyses, with measures at rest being strongly correlated to time-domain measures. Thus, in this series of participants, time- and frequency-domain analyses yielded similar interpretations.

Despite no overall group differences in time- or frequency-domain sympathetic transduction of BP, considerable interindividual variability was noted with individuals increasing or decreasing individual metrics across each stage of LBNP. Aligning with our prior data (11), these changes were strongly related to changes in the proportions of MSNA bursts firing above the OP. The mechanisms responsible for the changes in MSNA burst occurrence at different BP levels are unclear. LBNP increased the LF power and coherence of MSNA and BP, in agreement with previous work using similar or more intense levels (> 30 mmHg of negative pressure) (17, 18, 21). The increased BP-MSNA LF coherence is considered to be the result of increased MSNA burst clustering at troughs of BP oscillations (18). Despite these observations, the changes in MSNA burst firing above the OP were unrelated to sympathetic baroreflex sensitivity during LBNP. This observation is counterintuitive, as more bursts firing at higher BP levels should reduce the sympathetic baroreflex slope (or sensitivity). At −30 mmHg, LBNP increased the HF gain of both respiration-diastolic BP and respiration-MSNA, with the former associated with measures of sympathetic transduction. The latter finding suggests that participants with greater respiratory-driven changes in diastolic BP demonstrate a larger increase in diastolic BP following an MSNA burst during LBNP. This observation aligns with prior work in resting spontaneously breathing humans, which found lower MSNA burst incidence and sympathetic baroreflex sensitivity during high lung volume phases, associated with a greater proportion of beat-to-beat rises in diastolic BP (28). These data provide preliminary insight that respiratory input could be involved in modulating MSNA burst occurrence at higher levels of BP and the subsequent transduction response. The factors that determine changes in the firing of MSNA bursts relative to oscillations in BP require further investigation.

There are several alternative interpretations of the signal-averaged sympathetic transduction responses that warrant further discussion. It is well established that larger MSNA bursts (within and between participants) increase signal-averaged sympathetic transduction at rest (4, 25, 34). During LBNP, MSNA burst amplitude was increased without a concurrent increase in the diastolic BP response following MSNA bursts. This could be interpreted to demonstrate reduced sympathetic transduction (i.e., greater sympathetic outflow but the same BP response). One explanation for this finding pertains to LBNP-induced increases in the vasomotor set-points, which could alter BP responsiveness. For example, venous pooling in the lower extremities during LBNP decreases venous return and stroke volume, whereas resting BP is maintained by increased vascular resistance (16). Operating at higher prevailing vasomotor tones could augment the neurotransmitter release required to achieve similar sympathetic transduction responsiveness. However, this explanation fails to explain the LBNP-induced increase in low-frequency diastolic BP oscillations. Alternatively, in the absence of sympathetic activity (evaluated by the signal-averaged hemodynamic responses to cardiac cycles without

an MSNA burst), we observed larger reductions in diastolic BP during LBNP, suggesting a greater propensity for BP to fall during sympathetic quiescence. Although typically reported when conducting signal-averaged sympathetic transduction, the physiological significance and interpretation of hemodynamic responses to nonburst cardiac cycles are infrequently discussed. We previously suggested that using nonburst cardiac cycles as an internal baseline and assessing the difference between BP responses following MSNA may represent a more accurate measure of sympathetic transduction that is less affected by prevailing MSNA burst frequency (11). This measure along with the normalized sympathetic transduction metric both suggest that sympathetic transduction of BP is increased during LBNP. These findings are biologically plausible, as *1*) graded efferent stimulation of the sympathetic nervous system increases neurotransmitter efflux from sympathetic nerve terminals (3) resulting in larger sympathetic vasoconstrictor responses (38), and *2*) in resting humans, larger MSNA bursts or clusters of consecutive bursts are associated with higher signal-averaged sympathetic transduction of BP (8, 25, 34) and reductions in TVC (39). Thus, without concomitant nonneural compensatory changes, the effects of larger bursts of MSNA on subsequent BP responses should be greater during LBNP. Considering solely the BP response to MSNA bursts might fail to accurately quantify the sympathetic end-organ responsiveness but may be unmasked by considering hemodynamic responses to nonburst cardiac cycles.

Limitations

We acknowledge several methodological considerations. First, prior work has shown that more intensive levels of LBNP (>30 mmHg of negative pressure) can further augment BP and MSNA spectral power (17), which could potentially alter sympathetic transduction responses and the proportions of MSNA bursts firing above the OP. The current experimental approach of using low-to-moderate levels of LBNP was chosen to achieve sympathetic activation while minimally perturbing resting hemodynamics. Second, we were unable to measure spirometry-derived flow, which would be important for more accurately evaluating the impact of respiration on the proportion of bursts firings above the OP. Third, we did not assess the transduction of an MSNA burst on regional vascular conductance. Fourth, although no visible or audible shift in the MSNA signal occurred during LBNP, we cannot exclude the possibility of small shifts in the electrode, which could alter measurements of MSNA burst amplitude.

Perspectives and Significance

The current study demonstrates that acute baroreflex-mediated increases in MSNA using graded LBNP did not alter signal-averaged or frequency-domain measures of sympathetic transduction of diastolic BP or TVC. This result is explained by the observation that LBNP increased MSNA but did not alter the proportion of bursts firing above the OP and further evident by the strong relationships between interindividual sympathetic transduction responses and the proportion of bursts firing above the OP. In contrast, during LBNP, BP and TVC responses to nonburst cardiac cycles were progressively altered, and as a result, the differences between BP and TVC responses during MSNA burst and nonburst cardiac cycles were increased. This apparent increase in sympathetic transduction of BP would align with the increases in MSNA burst amplitude found during LBNP. Prior work at rest has consistently shown larger MSNA bursts to increase signal-averaged sympathetic transduction of BP (2, 25, 39). Further work is necessary to determine the most appropriate index for quantifying sympathetic transduction of BP in humans.

GRANTS

This research was supported by the Natural Science and Engineering Research Council of Canada (NSERC) Discovery Grant program (to P.J.M.), the Canada Foundation for Innovation (to P.J.M.), the Ontario Ministry of Research, Innovation and Science (to P.J.M.), and the American Physiological Society Arthur C. Guyton Award for Excellence in Integrative Physiology (to P.J.M.). P.J.M. is a recipient of an Early Researcher Award by the Ontario Ministry of Economic Development, Job Creation and Trade. M.N. was supported by the Canadian Institute of Health Research (CIHR) Frederick Banting and Charles Best Canada Graduate Scholarship.

DISCLOSURES

No conflicts of interest, financial or otherwise, are declared by the authors.

AUTHOR CONTRIBUTIONS

M.N. and P.J.M. conceived and designed research; M.N., C.K., A.L.T., J.B.L., J.C.B., and P.J.M. performed experiments; M.N. analyzed data; M.N. interpreted results of experiments; M.N. prepared figures; M.N. and P.J.M. drafted manuscript; M.N., C.K., A.L.T., J.B.L., J.C.B., and P.J.M. edited and revised manuscript; M.N., C.K., A.L.T., J.B.L., J.C.B., and P.J.M. approved final version of manuscript.

REFERENCES

1. **Carter JR.** Microneurography and sympathetic nerve activity: a decade-by-decade journey across 50 years. *J Neurophysiol* 121: 1183–1194, 2019. doi:10.1152/jn.00570.2018.
2. **Young BE**, **Greaney JL**, **Keller DM**, **Fadel PJ.** Sympathetic transduction in humans: Recent advances and methodological considerations. *Am J Physiol Heart Circ Physiol* 320: H942–H953, 2021. doi:10.1152/ajpheart.00926.2020.
3. **Vanhoutte PM**, **Verbeuren TJ**, **Webb RC.** Local modulation of adrenergic neuroeffector interaction in the blood vessel well. *Physiol Rev* 61: 151–247, 1981. doi:10.1152/physrev.1981.61.1.151.
4. **Nardone M**, **Incognito AV**, **Kathia MM**, **Omazic LJ**, **Lee JB**, **Teixeira AL**, **Xie S**, **Vianna LC**, **Millar PJ.** Signal-averaged resting sympathetic transduction of blood pressure: Is it time to account for prevailing muscle sympathetic burst frequency? *Am J Physiol Regul Integr Comp Physiol* 321: R484–R494, 2021. doi:10.1152/ajpregu.00131.2021.
5. **Robinson AT**, **Babcock MC**, **Watso JC**, **Brian MS**, **Migdal KU**, **Wenner MM**, **Farquhar WB.** Relation between resting sympathetic outflow and vasoconstrictor responses to sympathetic nerve bursts: Sex differences in healthy young adults. *Am J Physiol Regul Integr Comp Physiol* 316: R463–R471, 2019. doi:10.1152/ajpregu.00305.2018.
6. **Wallin BG**, **Nerhed C.** Relationship between spontaneous variations of muscle sympathetic activity and succeeding changes of blood pressure in man. *J Auton Nerv Syst* 6: 293–302, 1982. doi:10.1016/0165-1838(82)90002-9.
7. **Hissen SL**, **Macefield VG**, **Brown R**, **Taylor CE.** Sympathetic baroreflex sensitivity is inversely related to vascular transduction in men but not women. *Am J Physiol Heart Circ Physiol* 317: H1203–H1209, 2019. doi:10.1152/ajpheart.00501.2019.
8. **Berthelsen LF**, **Fraser GM**, **Simpson LL**, **Vanden Berg ER**, **Busch SA**, **Steele AR**, **Meah VL**, **Lawley JS**, **Figueroa-Mujíca RJ**, **Vizcardo-**

Galindo G, **Villafuerte F**, **Gasho C**, **Willie CK**, **Tymko MM**, **Ainslie PN**, **Stembridge M**, **Moore JP**, **Steinback CD.** Highs and lows of sympathetic neurocardiovascular transduction: influence of altitude acclimatization and adaptation. *Am J Physiol Heart Circ Physiol* 319: H1240–H1252, 2020. doi:10.1152/ajpheart.00364.2020.

9. **Petterson JL**, **O'Brien MW**, **Ramsay DJ**, **Johnston W**, **O'Neill CD**, **Dogra S**, **Mekari S**, **Floras JS**, **Kimmerly DS.** Sympathetic neurohemodynamic transduction is attenuated in older males independent of aerobic fitness. *Clin Auton Res* 32: 73–76, 2022. doi:10.1007/s10286-021-00845-y.
10. **Kobetic MD**, **Burchell AE**, **Ratcliffe LEK**, **Neumann S**, **Adams ZH**, **Nolan R**, **Nightingale AK**, **Paton JFR**, **Hart EC.** Sympathetic-transduction in untreated hypertension. *J Hum Hypertens* 36: 24–31, 2022. doi:10.1038/s41371-021-00578-5.
11. **Nardone M**, **Katerberg C**, **Incognito AV**, **Teixeira AL**, **Vianna LC**, **Millar PJ.** Blood pressure oscillations impact signal-averaged sympathetic transduction of blood pressure: Implications for the association with resting sympathetic outflow. *Am J Physiol Heart Circ Physiol* 321: H798–H806, 2021. doi:10.1152/ajpheart.00422.2021.
12. **Nardone M**, **Millar PJ.** Lower sympathetic transduction of blood pressure in uncontrolled hypertensives: physiological adaptation, methodological limitation, or both? *J Hum Hypertens* 36: 423–424, 2022. doi:10.1038/s41371-021-00638-w.
13. **Nardone M**, **Vianna LC**, **Millar PJ.** Reply to Fadel et al. *Am J Physiol Regul Integr Comp Physiol* 322: R123–R125, 2022. doi:10.1152/ajpregu.00265.2021.
14. Sympathetic transduction: Let's not forget about the physiology. *Am J Physiol Regul Integr Comp Physiol* 321: R634–R635, 2021. doi:10.1152/ajpregu.00212.2021.
15. **Steele AR**, **Berthelsen LF**, **Fraser GM**, **Phillips DB**, **Fuhr DP**, **Wong EYL**, **Stickland MK**, **Steinback CD.** Blunted sympathetic neurovascular transduction is associated to the severity of obstructive sleep apnea. *Clin Auton Res* 31: 443–451, 2021. doi:10.1007/s10286-021-00784-8.
16. **Goswami N**, **Blaber AP**, **Hinghofer-Szalkay H**, **Convertino VA.** Lower body negative pressure: physiological effects, applications, and implementation. *Physiol Rev* 99: 807–851, 2018. doi:10.1152/physrev.00006.2018.
17. **Cooke WH**, **Rickards CA**, **Ryan KL**, **Kuusela TA**, **Convertino VA.** Muscle sympathetic nerve activity during intense lower body negative pressure to presyncope in humans. *J Physiol* 587: 4987–4999, 2009. doi:10.1113/jphysiol.2009.177352.
18. **Yang H**, **Cooke WH**, **Reed KS**, **Carter JR.** Sex differences in hemodynamic and sympathetic neural firing patterns during orthostatic challenge in humans. *J Appl Physiol* 112: 1744–1751, 2012. doi:10.1152/japplphysiol.01407.2011.
19. **Pagani M**, **Lombardi F**, **Guzzetti S**, **Rimoldi O**, **Furlan R**, **Pizzinelli P**, **Sandrone G**, **Malfatto G**, **Dell'Orto S**, **Piccaluga E.** Power spectral analysis of heart rate and arterial pressure variabilities as a marker of sympatho-vagal interaction in man and conscious dog. *Circ Res* 59: 178–193, 1986. doi:10.1161/01.RES.59.2.178.
20. **Furlan R**, **Porta A**, **Costa F**, **Tank J**, **Baker L**, **Schiavi R**, **Robertson D**, **Malliani A**, **Mosqueda-Garcia R.** Oscillatory patterns in sympathetic neural discharge and cardiovascular variables during orthostatic stimulus. *Circulation* 101: 886–892, 2000. doi:10.1161/01.cir.101.8.886.
21. **Ryan KL**, **Rickards CA**, **Hinojosa-Laborde C**, **Cooke WH**, **Convertino VA.** Arterial pressure oscillations are not associated with muscle sympathetic nerve activity in individuals exposed to central hypovolaemia. *J Physiol* 589: 5311–5322, 2011. doi:10.1113/jphysiol.2011.213074.
22. **Nardone M**, **Incognito AV**, **Millar PJ.** Evidence for pressure-independent sympathetic modulation of central pulse wave velocity. *J Am Heart Assoc* 7: e007971, 2018. doi:10.1161/JAHA.117.007971.
23. **Doherty CJ**, **King TJ**, **Incognito AV**, **Lee JB**, **Shepherd AD**, **Cacoilo JA**, **Slysz JT**, **Burr JF**, **Millar PJ.** Effects of dynamic arm and leg exercise on muscle sympathetic nerve activity and vascular conductance in the inactive leg. *J Appl Physiol* 127: 464–472, 2019. doi:10.1152/japplphysiol.00997.2018.
24. **Notay K**, **Seed JD**, **Incognito AV**, **Doherty CJ**, **Nardone M**, **Burns MJ**, **Millar PJ.** Validity and reliability of measuring resting muscle sympathetic nerve activity using short sampling durations in healthy humans. *J Appl Physiol* 121: 1065–1073, 2016. doi:10.1152/japplphysiol.00736.2016.
25. **Nardone M**, **Incognito AV**, **Teixeira AL**, **Cacoilo JA**, **Vianna LC**, **Millar PJ.** Effects of muscle sympathetic burst size and burst pattern on time-to-peak sympathetic transduction. *Appl Physiol Nutr Metab* 46: 790–796, 2021. doi:10.1139/apnm-2020-0721.
26. **Ando S**, **Dajani HR**, **Floras JS.** Frequency domain characteristics of muscle sympathetic nerve activity in heart failure and healthy humans. *Am J Physiol* 273: R205–R212, 1997. doi:10.1152/ajpregu.1997.273.1.R205.
27. **Briant LJB**, **Burchell AE**, **Ratcliffe LEK**, **Charkoudian N**, **Nightingale AK**, **Paton JFR**, **Joyner MJ**, **Hart EC.** Quantifying sympathetic neurohaemodynamic transduction at rest in humans: Insights into sex, ageing and blood pressure control. *J Physiol* 594: 4753–4768, 2016. doi:10.1113/JP272167.
28. **Nardone M**, **Teixeira AL**, **Incognito AV**, **Vermeulen TD**, **Shafer BM**, **Millar PJ**, **Foster GE.** Within-breath sympathetic baroreflex sensitivity is modulated by lung volume but unaffected by acute intermittent hypercapnic hypoxia in men. *Am J Physiol Heart Circ Physiol* 319: H213–H221, 2020. doi:10.1152/ajpheart.00296.2020.
29. **Holwerda SW**, **Carter JR**, **Yang H**, **Wang J**, **Pierce GL**, **Fadel PJ.** CORP: standardizing methodology for assessing spontaneous baroreflex control of muscle sympathetic nerve activity in humans. *Am J Physiol Heart Circ Physiol* 320: H762–H771, 2021. doi:10.1152/ajpheart.00704.2020.
30. **R Core Team.** R: *A Language and Environment for Statistical Computing*. Vienna, Austria: R Foundation for Statistical Computing. https://www.r-project.org/.
31. **Bates D**, **Mächler M**, **Bolker B**, **Walker S.** Fitting linear mixed-effects models using lme4. *J Stat Softw* 67: 1–48, 2015. doi:10.18637/jss.v067.i01.
32. **Kuznetsova A**, **Brockhoff PB**, **Christensen RHB.** lmerTest package: tests in linear mixed effects models. *J Stat Softw* 82: 1–26, 2017. doi:10.18637/jss.v082.i13.
33. **Lenth RV**, **Buerkner P**, **Herve M**, **Love J**, **Miguez F**, **Riebl H**, **Singmann H.** *emmeans: Estimated Marginal Means, aka Least-Squares Means*. https://CRAN.R-project.org/package=emmeans.
34. **Vianna LC**, **Hart EC**, **Fairfax ST**, **Charkoudian N**, **Joyner MJ**, **Fadel PJ.** Influence of age and sex on the pressor response following a spontaneous burst of muscle sympathetic nerve activity. *Am J Physiol Heart Circ Physiol* 302: H2419–H2427, 2012. doi:10.1152/ajpheart.01105.2011.
35. **Steinback CD**, **Fraser GM**, **Usselman CW**, **Reyes LM**, **Julian CG**, **Stickland MK**, **Chari RS**, **Khurana R**, **Davidge ST**, **Davenport MH.** Blunted sympathetic neurovascular transduction during normotensive pregnancy. *J Physiol* 597: 3687–3696, 2019. doi:10.1113/JP277714.
36. **Young BE**, **Holwerda SW**, **Vranish JR**, **Keller DM**, **Fadel PJ.** Sympathetic transduction in type 2 diabetes mellitus: Impact of statin therapy. *Hypertension* 74: 201–207, 2019. doi:10.1161/HYPERTENSIONAHA.119.12928.
37. **Simpson LL**, **Busch SA**, **Oliver SJ**, **Ainslie PN**, **Stembridge M**, **Steinback CD**, **Moore JP.** Baroreflex control of sympathetic vasomotor activity and resting arterial pressure at high altitude: insight from Lowlanders and Sherpa. *J Physiol* 597: 2379–2390, 2019. doi:10.1113/JP277663.
38. **Stauss HM**, **Kregel KC.** Frequency response characteristic of sympathetic-mediated vasomotor waves in conscious rats. *Am J Physiol Heart Circ Physiol* 271: H1416–H1422, 1996. doi:10.1152/ajpheart.1996.271.4.H1416.
39. **Fairfax ST**, **Padilla J**, **Vianna LC**, **Davis MJ**, **Fadel PJ.** Spontaneous bursts of muscle sympathetic nerve activity decrease leg vascular conductance in resting humans. *Am J Physiol Heart Circ Physiol* 304: H759–H766, 2013. doi:10.1152/ajpheart.00842.2012.